Effects of Hydrometeor Convergence on Precipitation Estimate and Prediction

Chung-Hsiung Sui
Institute of Hydrological Sciences, National Central University

Abstract

Effects of hydrometeor convergence on precipitation estimate and prediction are investigated using a 2-D cloud resolving model with the imposed forcing from the Tropical Ocean Global Atmosphere Coupled Ocean–Atmosphere Experiment (TOGA COARE). An analysis of vertically integrated budgets of water vapor and total clouds (or hydrometeors) through the troposphere is carried out within three areas: 96 km, 48 km, and 24 km. The analysis shows that the total moisture source due to surface evaporation and vertically integrated moisture convergence ($E_S + [CONV_{qv}]$) all converts into clouds through vapor condensation and deposition rates (SI_{qv}). But only a portion of SI_{qv} (or total moisture source) reaches ground as surface rainfall rate (P_s). The ratio of P_s to either total moisture source or SI can be defined as precipitation efficiency. The latter is termed cloud microphysics precipitation efficiency (CMPE= P_s / SI_{qv}).Apparently, the precipitation efficiency relative to the total moisture source is statistically equivalent to CMPE. The calculation of vertically integrated cloud budget shows that the CMPE can be larger than 100 % as a result of hydrometeor convergence from the neighboring atmospheric columns. This is most evident in light-rain conditions (<5 mm hr^{-1} for 96- and 48-km domains and <10 mm hr^{-1} for 24-km domain). On the other hand, CMPE is normally smaller than 100% in cases of heavy-rains (>5 mm hr^{-1}) associated with hydrometeor divergence. The hydrometeor divergence (convergence) in heavy (light) rain conditions is associated with the mesoscale circulation that transport hydrometeors generated in the convective cells at the front to the trailing stratiform-rain regions. Clearly, hydrometeor convergence needs to be included in quantitative precipitation estimate/forecast (QPE/F) using numerical models. This is expected to be more crucial in strong convective systems like hurricanes/typhoons and topography-induced convection. The study also indicates a need to include a prognostic cloud microphysics parameterization scheme in models to predict the formation and transport of hydrometeors.

1. Introduction

The current study is led by two key questions: How important is the horizontal cloud transport in prediction of surface rain rate? Does it depend on the strength of convection? The goal of this study is to answer the above questions using a cloud resolving model. The model and forcing are discussed in Section 2. The vertically integrated budgets of water vapor and clouds are estimated in Section 3. The importance of horizontal cloud advection in the prediction of the surface rain rate is examined in Section 4. A summary is given in Section 4.

2. Model and experiment

The cloud-resolving model was originally developed by Soong and Ogura (1980), Soong and Tao (1980) and Tao and Simpson (1993). The 2-D version of the model used by Sui et al. (1994, 1998) and further modified by Li et al. (1999) is used in this study. The details of the model including cloud microphysics parameterization schemes are referred to Li et al. (1999). The experiment analyzed in this study is conducted with the model forced by the zonally uniform vertical velocity, zonal wind, and thermal and moisture advections, which are derived by Professor Minghua Zhang and his research group at the State University of New York at Stony Brook, based on the 6-hourly TOGA COARE observations within the Intensive Flux Array (IFA) region (Zhang, personal communication, 1999). The calculations are based on the constrained variational method on column-integrated budgets of mass, heat, moisture and momentum proposed by Zhang and Lin (1997). Hourly sea surface temperature at the Improved Meteorological (IMET) surface mooring buoy (1.75°S, 156°E) (Weller and Anderson 1996) is also imposed in the model. The model is integrated from 0400 LST 19 December 1992 to 0400 LST 9 January 1993 (21 days total). The horizontal domain is 768 km. The grid mesh of 1.5 km and the time step of 12 seconds are used in model integrations.

An analysis of the hourly simulation data within a 36-hour period (0000 LST 20-1200 LST 21 December 1992) is presented in the current study. The same analysis is also applied to the hourly data of the 21-day period, and the conclusion remains unchanged.

3. Vertically integrated water budgets

The vertically-integrated water vapor and total cloud budgets can be expressed as:

$$\partial[q_v]/\partial t = [CONV_{qv}] + E_S - SI_{qv} + SO_{qv}, \quad (1)$$

$$\partial[C]/\partial t = [CONV_C] - P_S + S_C \cdot \quad (2)$$

where $[F]=\int_0^{zt} \bar{\rho} F dz$ for any variable F, q_v the mixing ratio of water vapor, $[CONV_{qv}]$ moisture convergence, $E_S = \bar{\rho}(w'q_v')_S$ surface evaporation, $SI_{qv} = [P_{CND}] + [P_{DEP}] + [P_{SDEP}] + [P_{GDEP}]$ the sum of vapor condensation rate

($[P_{CND}]$), vapor deposition rates for growth of cloud ice ($[P_{DEP}]$), snow ($[P_{SDEP}]$) and graupel ($[P_{GDEP}]$), SO_{qv}= $[P_{REVP}]$+ $[P_{MLTG}]$+ $[P_{MLTS}]$ the sum of growth of vapor by evaporation of raindrop ($[P_{REVP}]$), melting graupel ($[P_{MLTG}]$), melting snow ($[P_{MLTS}]$), $C = \sum q_i$ the sum of mixing ratio of cloud water (q_c), raindrop (q_r), cloud ice (q_i), snow (q_s), and graupel (q_g), $[CONV_C]$ hydrometeor convergence, surface rain rate $P_s = \overline{\rho}(w_{TV}C)_S$ w_{TV} terminal velocity of each cloud species, $S_C = -SO_{qv} + SI_{qv}$. Note that $[CONV_{qv}] = -[\overline{u}^o \times \partial \overline{q}_v^o / \partial x] - [\overline{w}^o \times \partial \overline{q}_v / \partial z]$ and $[CONV_C] = 0$ when averaged over the whole domain under the cyclic boundary condition. Here $\overline{u}^o$ and $\overline{w}^o$ are imposed zonal and vertical winds; x and z are zonal and vertical coordinates. Details of the microphysical terms are described in Li et al. (1999, 2002c).

The budgets (1) and (2) and relevant dominant microphysical terms are schematically shown in Fig. 1. The dominant terms are identified based on the study of Li et al. 2002c) and the domain- and time-averaged budgets of water vapor and total clouds of the current experiment. The budget shows that most of the total moisture source ($CONV_{qv}$+E_s) are used to form cloud water and cloud ice through vapor condensation [P_{CND}/ ($CONV_{qv}$+E_s)= 83%] and deposition [P_{DEP}/($CONV_{qv}$+E_s) = 14%]. The conversion of cloud water to precipitation occurs primarily through collection of cloud water by rain below the freezing level (P_{RACW}/P_{CND} = 66%) and through riming of cloud water onto precipitating ice (snow and graupel) above the freezing level [(P_{GACW} + P_{SACW})/ P_{CND} = 31%]. The melting of precipitating ice (P_{SMLT} , P_{GMLT}) mainly compensates the evaporation of rain (P_{REVP}). The collection efficiency (P_{RACW}/P_{CND} = 66%) accounts for the precipitation efficiency [P_s/ ($CONV_{qv}$+E_s)= 65%].

In the following, vertically integrated budgets of water vapor and total clouds are analyzed within three areas: 96, 48, and 24 km. Figure 2 shows the values of SI_{qv} versus the values of total moisture source averaged within the three areas. The two variables have very similar variations. The root mean square differences between the two variables are less than 1.3, 1.8 and 2.5 mmh^{-1} for 96-, 48-, and 24-km cases, respectively, and their linear correlation coefficients are about 0.89 for all the three cases, which is well above 95% confidence level. This indicates that

$$[P_{CND}]+[P_{DEP}]+[P_{SDEP}]+[P_{GDEP}] \approx E_s + [CONV_{qv}] \quad (3)$$

is a valid approximation in different area averages.

4. Precipitation efficiency

The relation (3) supports the basic premise of Kuo's cumulus parameterization (1974). However, what portion of the net vapor condensation and deposition rate converts into surface rainfall rate is central to the cumulus parameterization. This can be expressed by "precipitation efficiency". Here we introduce two definitions of precipitation efficiency. One is the cloud microphysics precipitation efficiency (CMPE),

$$\text{CMPE} = \frac{P_s}{SI_{qv}} = 1 - \frac{SO_{qv}}{SI_{qv}} + \frac{[CONV_C]}{SI_{qv}}. \quad (4)$$

In (4), the storage term of clouds is neglected. The CMPE is defined as the ratio of surface rain rate to the sum of vapor condensation rate, vapor deposition rate for growth of cloud ice, snow and graupel (SI_{qv}). Notice the CMPE defined here is different from that defined in Li et al. (2002b) since additional terms ($[P_{SDEP}] + [P_{GDEP}]$) may be important for mesoscale calculations.

The other is moisture convergence precipitation efficiency (MCPE),

$$\text{MCPE} = \frac{P_s}{[ADV_{qv}] + E_s} = \frac{P_s}{SI_{qv} - SO_{qv} + \partial[q_v]/\partial t} \quad (5)$$

MCPE is defined as the ratio of surface rain rate to the sum of surface evaporation and vertically integrated horizontal and vertical moisture advection. MCPE defined here is identical to LSPE in Li et al. (2002b) when the MCPE is calculated using domain-mean quantities. In (5), the magnitudes of $(SO_{qv} - \partial[q_v]/\partial t)$ is statistically much smaller than the magnitude of SI_{qv} as shown in Fig. 2. This is consistent with the finding that the sum of vapor condensation rate, vapor deposition rate for growth of cloud ice, snow and graupel is close to the sum of surface evaporation and vertically integrated horizontal and vertical moisture advection. As a result, CMPE and MCPE are statistically interchangeable.

The definition of CMPE in (4) indicates that the values of CMPE can be larger than one if $[CONV_c]$ is positive through the advection of clouds into the region of interest. This is indeed observed in Figure 3 that shows the CMPE versus surface rain rate. The figure shows that, while most of the CMPE values are smaller than 100 %, the values of CMPE > 100 % do exist in light-rain conditions (surface rain rates are smaller than 5 mmh^{-1} for 96- and 48-km cases and smaller than 10 mm h^{-1} for 24-km case). Although the data are scattered, the CMPE tends to approach to a threshold value (5 mmh^{-1} for 96- and 48-km averages and 10 mmh^{-1} for 24-km averages) with increasing surface rain rate.

The values of CMPE larger than 100 % represent those cases with surface rain rate larger than the total vapor condensation and deposition rates. This requires a positive hydrometeor convergence to balance the cloud budget [see equation (2) above]. Indeed an inspection of the plot of hydrometeor convergence versus CMPE (Fig. 4) shows that most CMPEs larger than 100 % are associated with positive hydrometeor convergence. This is a clear evidence that the cases of CMPE > 100 % are caused by adding hydrometeors from the neighboring atmospheric columns. Figure 4 also displays the effects of hydrometeor divergence (mostly negative advection) on the surface rain rate when the CMPE is smaller than 100 %. The above results indicate a significant effect of hydrometeor convergence on surface precipitation distribution.

The dependence of CMPE on the rainfall intensity can be explained by the mesoscale-flow patterns in the convective and stratiform rain regions of the squall line that is the most dominant features of cloud clusters simulated by 2D cloud resolving models as reported in many previous studies (e.g. Sui et al. 1994, Yang and Houze 1995, Tao et al. 1993, Peng et al. 2001). A

composite of simulated cloud clusters by Peng et al. (2001) is shown in Fig. 5. The simulated cloud cluster is very similar to a conceptual model of squall line constructed by Houze et al. (1989) based on observations. The mesoscale flow is characterized by front-to-rear inflow at low and middle levels, ascending slantwise front-to-rear flow, and descending rear inflow. Gust-front type of new cells generate at the front while older cells are advected rearward in the sloping flow. The mesoscale circulation transports hydrometeors generated in new convective cells at the leading edge of the mesoscale system to the trailing stratiform clouds regions, resulting a hydrometeor divergence in the regions of heavy convective showers, and a hydrometeor convergence in the regions of stratiform rain where descending rear inflow also contributes to a hydrometeor convergence.

5. Conclusions and discussions

The impacts of hydrometeor convergence on precipitation distribution at surface is examined using a 2-D cloud resolving simulation with the imposed forcing from the TOGA COARE. The analysis of root mean square difference and linear correlation coefficients shows that the sum of vapor condensation rate (P_{CND}), vapor deposition rates for growth of cloud ice (P_{DEP}), snow (P_{SDEP}) and graupel (P_{GDEP}) is approximately balanced by the sum of surface evaporation (E_s) and vertically integrated moisture convergence, indicating that the total moisture source in the atmospheric column is converted into clouds. This is a basis of cumulus parameterization scheme of Kuo (1965, 1974). The relation leads to the statistical equivalence of precipitation efficiencies defined by cloud microphysics [CMPE = $P_s / (P_{CND}+P_{DEP}+P_{SDEP}+P_{GDEP})$] and by total moisture source [MCPE = $P_s / (E_s+CONV_{qv})$].

The precipitation efficiency larger than 100 % occurs in light-rain conditions (<5 mm hr^{-1}) as a result of the additional hydrometeor converging into the atmospheric column. On the other hand, a loss of clouds due to hydrometeors diverging out to the neighboring columns requires the CMPE to be smaller than 100 %. This occurs mostly in heavy-rain conditions (>5 mm hr^{-1}). The dependence of CMPE on the rainfall intensity can be explained by the mesoscale-flow patterns in the convective and stratiform rain regions of the squall line. Since the mesoscale precipitating features (like squall lines) and associated circulation can be considered fairly representative of tropical as well as mid-latitude cases, the effect of horizontal hydrometeor advection on the precipitation generation and distribution discussed in this study is expected to be more important in severe weather events like hurricanes/typhoons that has spiral rainbands and very strong mesoscale circulation. As a result, an accurate estimate/prediction of surface rainfall distribution produced by organized convective events must consider hydrometeor convergence. This can only be done by including prognostic equations of cloud hydrometeors in the numerical models used for quantitative precipitation estimate/forecast (QPE/F).

References

Houze, R. A., Jr, S. A. Rutledge, M. I. Biggerstaff, and B. F. Smull, 1989: Interpretation of Doppler weather radar displays of midlatitude mesoscale convective systems. *Bull. Amer. Meteor. Soc.*, **70**, 608-620.

Kuo, H. L., 1974: Further studies of the parameterization of the influence of cumulus convection on large-scale flow. *J. Atmos. Sci.*, **31**, 1232-1240.

Li, X., C.-H. Sui, K.-M. Lau, and M.-D. Chou, 1999: Large-scale forcing and cloud-radiation interaction in the tropical deep convective regime. *J. Atmos. Sci.*, **56**, 3028-3042.

Li, X., C.-H. Sui, and K.-M. Lau, 2002b: Precipitation efficiency in the tropical deep convective regime: A 2-D cloud resolving modeling study. *J. Meteor. Soc. Japan*, **80**, 205-212.

Li, X., C.-H. Sui, and K.-M. Lau, 2002c: Dominant cloud microphysical processes in a tropical oceanic convective system: A 2-D cloud resolving modeling study. *Mon. Wea. Rev.*, in press.

Peng, L., C.-H. Sui, K.-M. Lau, and W.-K. Tao, 2001: Genesis and evolution of hierarchical clouds clusters in a two-dimensional cumulus-resolving model. *J. Atmos. Sci.*, **58**, 877-895.

Soong, S. T., and Y. Ogura, 1980: Response of tradewind cumuli to large-scale processes. *J. Atmos. Sci.*, **37**, 2035-2050.

Soong, S. T., and W.-K. Tao, 1980: Response of deep tropical cumulus clouds to Mesoscale processes. *J. Atmos. Sci.*, **37**, 2016-2034.

Sui, C.-H., K.-M. Lau, W.-K. Tao, and J. Simpson, 1994: The tropical water and energy cycles in a cumulus ensemble model. Part I: Equilibrium climate. *J. Atmos. Sci.*, **51**, 711-728.

Sui, C.-H., X. Li, and K.-M. Lau, 1998: Radiative-convective processes in simulated diurnal variations of tropical oceanic convection. *J. Atmos. Sci.*, **55**, 2345-2359.

Tao, W.-K., and J. Simpson, 1993: The Goddard Cumulus Ensemble model. Part I: Model description. *Terr. Atmos. Oceanic Sci.*, **4**, 35-72.

Tao, W.-K., J. Samson, C.-H. Sui, S. Lang, J. Scala, B. Ferrier, M. D. Chou and K. Pickering, 1993: Heating, moisture and water budgets in the convective and stratiform regions of tropical and mid-latitude squall lines: their sensitivity to longwave radiation. *J. Atmos. Sci.* **50**, 673-690.

Yang, M.-J., and R. A. Houze, Jr. 1995: Sensitivity of squall-line rear inflow to ice microphysics and environmental humidity. *Mon. Wea. Rev.* ,**123**, 3175-3193.

Zhang, M. H., and J. L. Lin, 1997: Constrained variational analysis of sounding data based on column-integrated budgets of mass, heat, moisture, and momentum: Approach and application to ARM measurements. *J. Atmos. Sci.*, **54**, 1503-1524.

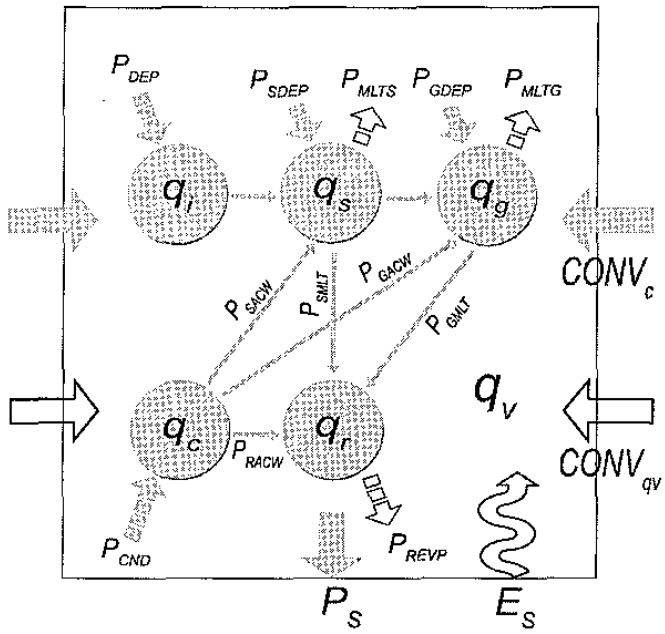

Fig. 1 A schematic diagram for the vertically integrated water vapor and total cloud budgets with dominant microphysics terms identified based on Li et al. 2002c and current experiment.

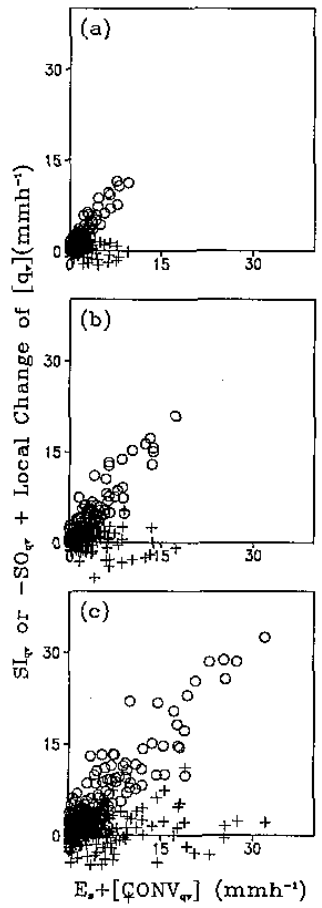

Fig. 2 SI_{qv} (circle) and $-SO_{qv} + \frac{\partial[q_v]}{\partial t}$ (cross) versus E_s+[$CONV_{qv}$] averaged within (a) 96 km, (b) 48 km, and (c) 24 km. Unit is mmh^{-1}.

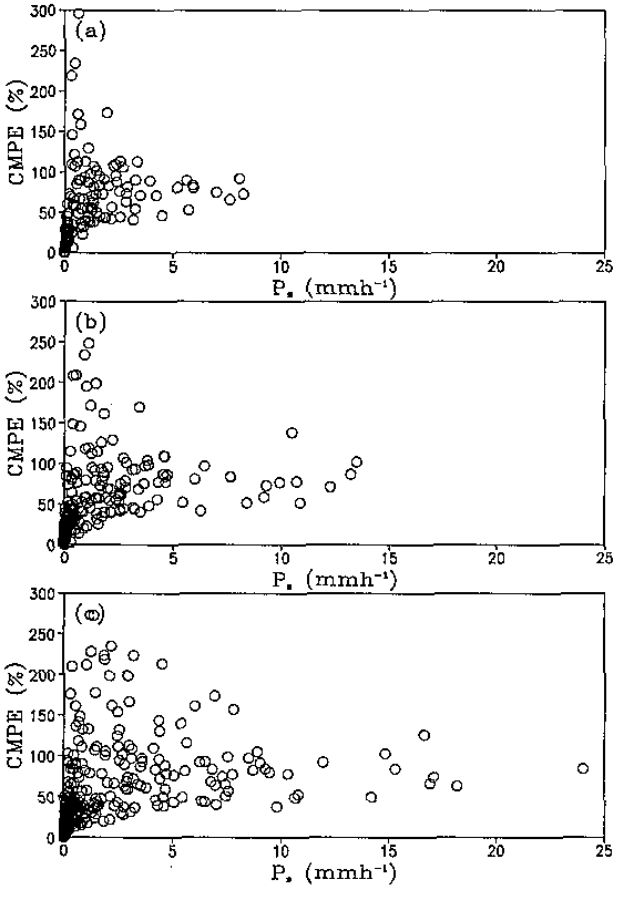

Fig. 3 CMPE (%) versus Ps (mmh^{-1}) averaged within (a) 96 km, (b) 48 km, and (c) 24 km.

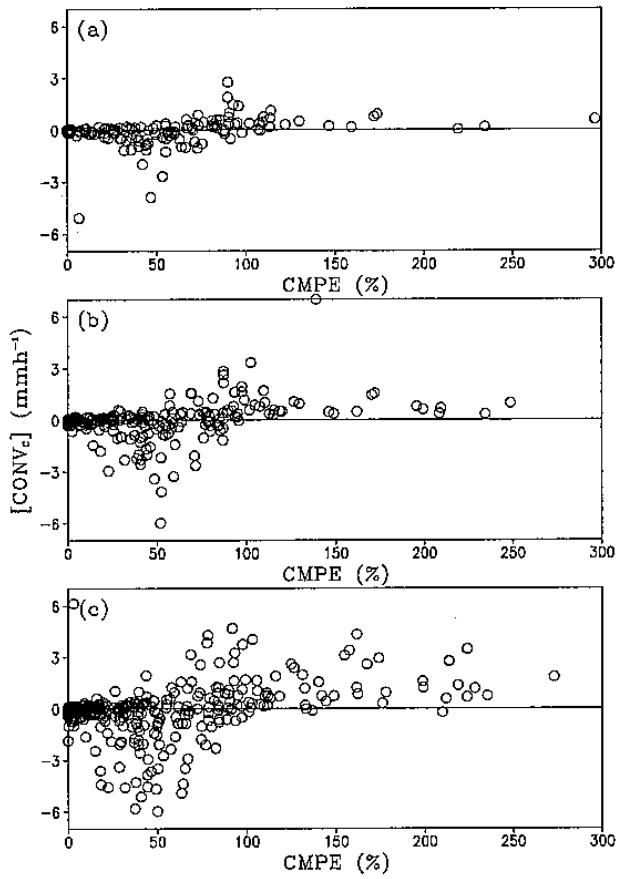

Fig. 4 [CONV$_C$] (mmh^{-1}) versus CMPE (%) averaged within (a) 96 km, (b) 48 km, and (c) 24 km.

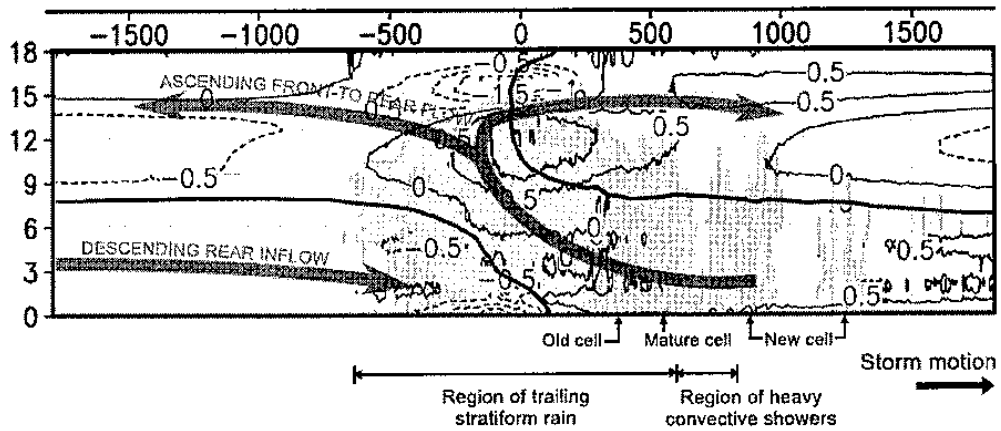

Fig. 5. Composite of cloud clusters relative to the convection center as simulated by Peng et al. (2001). The mesoscale circulation is drawn based on perturbation zonal and vertical velocities as represented by thick arrows (zero perturbation zonal velocity are denoted by thick contours). Areas of total cloud content >0.05 g kg^{-1} are shaded. The perturbation temperature (thin contours) and humidity (similar to perturbation temperature, not shown) generate an asymmetric mass distribution such that the surface pressure is low in the front and high in the rear. The perturbation thermal structure signals an internally heated mode-1 gravity wave. The composite structure is similar to the conceptual model of a squall line with a trailing stratiform area in a vertical cross section oriented perpendicular to the convective line as constructed by Houze et al. 1989.